DISTINCTIVE SPATIAL CONFIGURATION OF A CLASS OF MICROWAVE FLARING SOURCES

M. R. Kundu[1] and V. I. Garaimov[1]

[1]*Astronomy Department, University of Maryland, College Park, MD 20742*

ABSTRACT

We discuss a class of microwave flares whose source regions exhibit a distinctive spatial configuration; the primary energy release in these flares results from the interaction between emerging magnetic flux and an existing overlying region. Such events typically exhibit radio, X-ray and EUV emission at the main flare site (the site of interaction) and in addition radio emission at a remote site up to 1×10^5 km away in another active region. We have identified and studied more than a dozen microwave flares in this class, in order to arrive at some general conclusions on reconnection and energy release in such solar flares. Typically, these flares show a gradual rise showing many subsidiary peaks in both radio and hard X-ray light curves with a quasi-oscillatory nature with periods of 5-6 seconds, a bright compact X-ray& EUV emitting loop in the main flare source, a delay of the radio emission from the remote source relative to the main X-ray-emitting source. The magnetic field in the main flare site changes sharply at the time of the flare, and the remote site appears to be magnetically connected to the main flare site.

INTRODUCTION

It has been known for a long time that flares occur in regions consisting of many magnetic loops. The multiple magnetic loop configuration of flaring regions has led to the suggestion that at least in some cases a flare is caused by the interaction between loops. Interactions between newly emerging flux and overlying magnetic fields have been known to cause flares. A two-dimensional reconnection model of such flares was developed by Heyvaerts et al (1977) and it has been used in the past to interpret the onset of flares in various spectral domains.

In the past, Kundu et al (1982), and Kundu and Shevgaonkar (1984) used VLA observations of two flares observed at 5 and 15 GHz with a few arcsecond spatial resolution, and interpreted the intensity and polarization maps of the flaring regions in terms of reconnection between newly emerging flux and the pre-existing flux or overlying magnetic field. More recently, Hanaoka(1996,1997,1999a) analyzed a relatively large number of flares using Nobeyama Radioheliograph (NoRH) data along with Yohkoh SXT and Kitt Peak Natioanl Observatory magnetogram data. He found that emerging flux appeared near one sunspot-dominated active region, and argued that the interactions between this emerging flux and the overlying loop resulted in the onset of flares and microflares, although he did not have magnetogram data available with sufficient cadence to test this idea thoroughly. The main flare site in each case was the location of emerging flux, which also happened to be the site of enhanced soft X-ray and EUV brightening. The NoRH images showed that at 17 GHz a compact brightening occurred at the main flare site as well as a brightening near a remote region of opposite polarity. Hanaoka(1999b) further showed that the 17 GHz brightenings in the remote sources (separated from the main flare sites by as much as $\leq 10^5$ km) were delayed by some fractions of a second, implying that high energy electrons produced at the main flare site propagated over to the remote site.

In this paper, we discuss general characteristics of the class of flares based on the analysis of several flares

Table 1. List of selected flares

Event date	Time UT	Radio data NoRH	Other data	Location (NOAA)	Separation of remote site
Oct.25, 1999	06:28	17GHz 34GHz	Yohkoh (HXT,SXT) SOHO (EIT,MDI) TRACE	S26E36(8741) S12E16(8739)	120 000km
Nov.16, 1999	04:08	17GHz 34GHz	SOHO (EIT,MDI)	N16W68(8758)	140 000km
Jul.09, 1999	22:38	17GHz 34GHz	Yohkoh (HXT,SXT) SOHO (EIT,MDI)	N21W66	70 000km
Jul.02, 1999	01:33	17GHz 34GHz	Yohkoh (HXT,SXT) SOHO (EIT,MDI) TRACE	S25E06(8611)	74 000km
Mar.14, 1999	01:23	17GHz 34GHz	Yohkoh (SXT) SOHO (EIT,MDI)	N15E38(8487)	68 000km
Dec.14, 1994	05:41	17GHz	Yohkoh (HXT,SXT)	S10W07(7815)	77 000km
Jun.7, 1993	05:49	17GHz	Yohkoh (HXT,SXT)	S09W30(7518)	61 000km
Apr.10, 1993	23:35	17GHz	Yohkoh (HXT,SXT)	S08W51(7469)	69 000km
Feb.6, 1993	05:27	17GHz	Yohkoh (HXT,SXT)	S09E67(7420)	61 000km

(presented in table 1) which exhibit a similar magnetic field topology. The flare produces activity in two active regions separated by a large distance (10^5 km). The main flaring region (i.e., the region of the most intense emission at EUV, X-ray and radio wavelengths) contains a compact loop. We use data from a large number of sources: ground-based data from Nobeyama Radio Heliograph (NoRH) and space data from the satellites SOHO, Yohkoh, and TRACE to study these flares involving both large and small loop systems and address the issues of how the two loop systems interact and what the possible triggers of the interaction are. In addition, some events feature oscillations in X-ray and radio emissions which provide an additional constraint on physical parameters. High-cadence magnetogram data allowed us to confirm the changes in the magnetic field that existed prior to the flare.

GENERAL CHARACTERISTICS OF THIS CLASS OF FLARES

The following properties appear to be common to many events of this class, which we illustrate by using examples of July 02, 1999 event (Fig. 1), March 14, 1999 event (Fig. 2), Nov.16, 1999 event (Fig. 3) and Oct.25, 1999 event (Fig. 4) :

1. The light curves show a relatively slow rise in both hard X-rays and microwaves (fig. 1a).
2. Both hard X-ray and radio light curves show many quasi-periodic oscillations (fig. 1a).
3. Radio images show two sources separated by a large distance: for Oct 25 (fig. 4a), the two sources are in different active regions 160" apart. Only one of the sources would be identified as the flare site at other wavelengths (e.g., a bright loop is observed at the main flare site at EUV wavelengths). The remote source is not prominent at any other wavelength (e.g., soft X-rays, EUV).
4. Both radio sources show oscillations,specially during the rise phase of the flare (fig. 3c,4c).
5. The magnetic field appears to be stronger at the remote source and the radio polarization is higher than at the main flare site.
6. The dominant radio polarizations in the main and remote sources are of opposite sense.
7. The main radio source is generally bipolar, indicating a compact flaring loop.

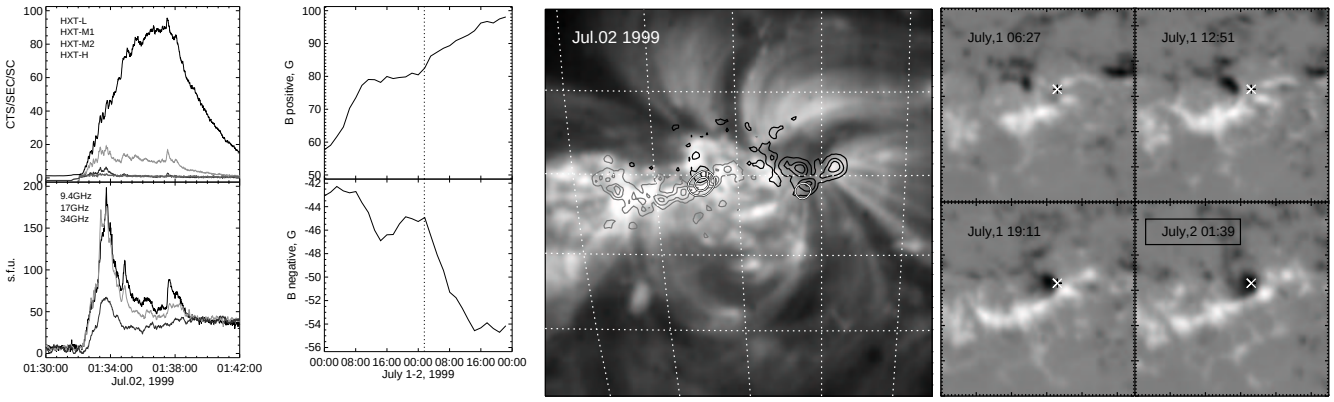

Fig. 1. Time profiles and images of July 2, 1999 event: a)time profiles of hard X-rays in all Yohkoh/HXT channels and in microwaves [left panel]; b) time variations of the magnetic flux averaged over the main flare site (the area shown in Fig. 1d); c) contours of 17GHz image(white line) and MDI image (gray and black line) superposed onto the EIT 195Å image; d)a sequence of the magnetograms from July 1, 06:27UT to July 2, 01:39UT [right panel].

8. The radio emission from the remote source is delayed with respect to the main source, with the delay corresponding to apparent velocities of order $1 - 2 \times 10^5$ km s^{-1} (fig. 3c,4c).

It is striking that events selected on purely morphological grounds (two well-separated sources in the 17 GHz images, with only one showing bright X-ray emission; Hanaoka 1997) show so many similarities in other properties. We note that the selection based on the presence of two well-separated radio sources introduces a selection effect which favors a stronger magnetic field at the remote source. In any event where the remote source does not lie in a stronger field the radio emission from the remote source is probably not detectable at 17 GHz because the number of nonthermal electrons is lower in the remote source than in the main source, and they radiate less strongly because optically-thin gyrosynchrotron emissivity is proportional to a high power of the magnetic field strength (e.g., $\propto B^{3.4}$ for an E^{-4} energy distribution: Dulk and Marsh 1982).

MAGNETIC EVOLUTION OF PRE-FLARE REGIONS AND MAGNETIC CONNECTIVITY BETWEEN MAIN FLARE SITE AND REMOTE REGION

In order to understand the magnetic field evolution of the flaring region, we have studied MDI images for two days prior to and including the pre-flare, and post-flare phases with a cadence of about 96 minutes. Inspection of a magnetogram movie shows movement of the isolated emerging magnetic field feature near the main flare site. To show these changes with stationary images, we present in Figure 1d a sequence of magnetograms for flaring region. We use black-white cross labels to provide stationary reference points. Also in Fig. 1b we present time profile of the average strength of the magnetic field, for each magnetic polarity separately. For each event there was a monotonic change of the average magnetic field of one polarity along with a sharp change of the field just prior to the flare occurrence.

The remote flaring region is observed only in microwaves (17 and 34 GHz). To understand the magnetic connection between the two regions and the possible role of the remote region in the flare we used images of the active region from EIT, TRACE, and SXT. Inspection of figure 1c shows that there is a connection of the main flare site with the remote radio source by the loop observed on EIT image.

As can be seen in Fig. 4a, for the event of Oct. 25, 1999 there are two possible magnetic connections between AR 8741 and AR 8739. Both sets of loops are evident in EIT images acquired just before the flare and show roughly equal brightness at that time. For details of Oct. 25, 1999 event, see Kundu et al (2001).

THE OSCILLATIONS

One of the characteristics of this class of microwave events is that their time profiles seem to exhibit oscillations in both hard X-ray and microwave bands.

We find that there is extremely good correlation between the HXT L and M1 channels, HXT M1 and

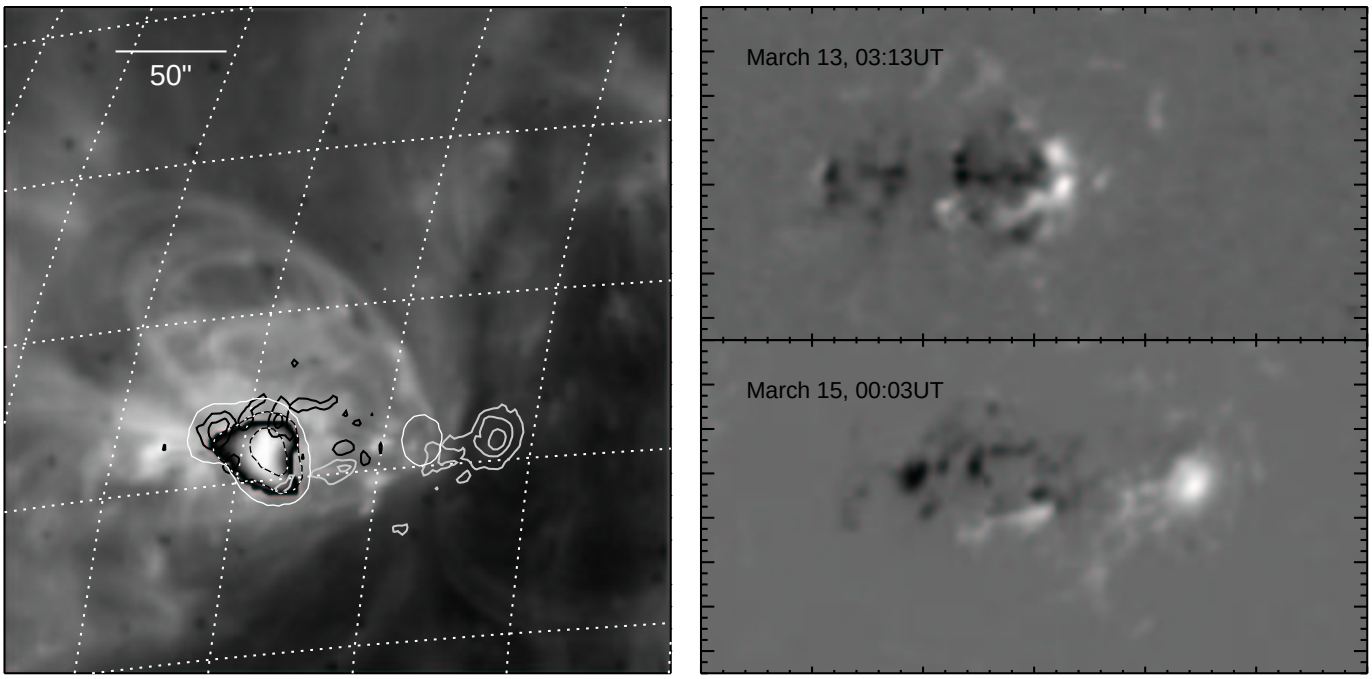

Fig. 2. Images of March 14, 1999 event: a)contours of 17GHz image (white line), 34GHz image (black dash line) and MDI image (gray and black line) superposed onto the EIT 195Å image with embedded soft X-ray image of the main flaring loop[left panel]; b)two MDI images of the flare site before and after the flare occurred [right panel].

M2 channels, HXT L channel and 17 GHz south source, and HXT M1 channel and 17 GHz south source respectively (Fig. 1a). Such good correlations suggest that emissions in hard X-rays and at 17 GHz in the southern source are similar in nature and the same electron population is responsible for these emissions.

Oscillations may reflect the characteristic frequency of some structure in the corona and thus can be used to infer physical properties of coronal structures. In such events, there is the additional involvement of loops with two very different lengths, and the question of whether the oscillations appear on both loop systems. Since the oscillation period reflects a resonance in a particular structure, two structures with different sizes should have very different oscillation periods. The presence of the same oscillation period in large and small loops would imply that one structure is the source of the radiating particles in both sets of loops. Oscillations visible simultaneously in microwaves and hard X-rays can be due to modulation of the magnetic tube width by a disturbance moving across the loop at the Alfvén speed. The oscillation period allows us to determine the density in the flare loop under the assumption that the oscillation period corresponds to transverse oscillations of the loop at the Alfvén speed.

Figure 4c shows part of the time profile of 17GHz emission from the main and the remote sources for Oct.25, 1999 event. Inspection of this figure indicates that, at least in the rise phase, the radio light curves of the main and remote sources behave similarly. Note that the time profile of the remote sources has been delayed by 0.95 s for this event.

This delay of the remote source is a clear indication that nonthermal electrons producing the radio emission are accelerated in the main flare site and then propagate to the remote site along magnetic field lines. We follow Hanaoka (1999a) and use the 0.95 s delay of the remote source to estimate the electron energy. The measured distance between the sources is 1.2×10^5 km, giving an apparent velocity of 1.3×10^5 km s^{-1}, which is very close to the values deduced for several flares by Hanaoka(1999b).

CONCLUSIONS

1. Multiwavelength studies of this class of impulsive flares has permitted us to clarify the manifestations and properties of multiple loop configurations of complex flaring sources. We suggest that a flare could

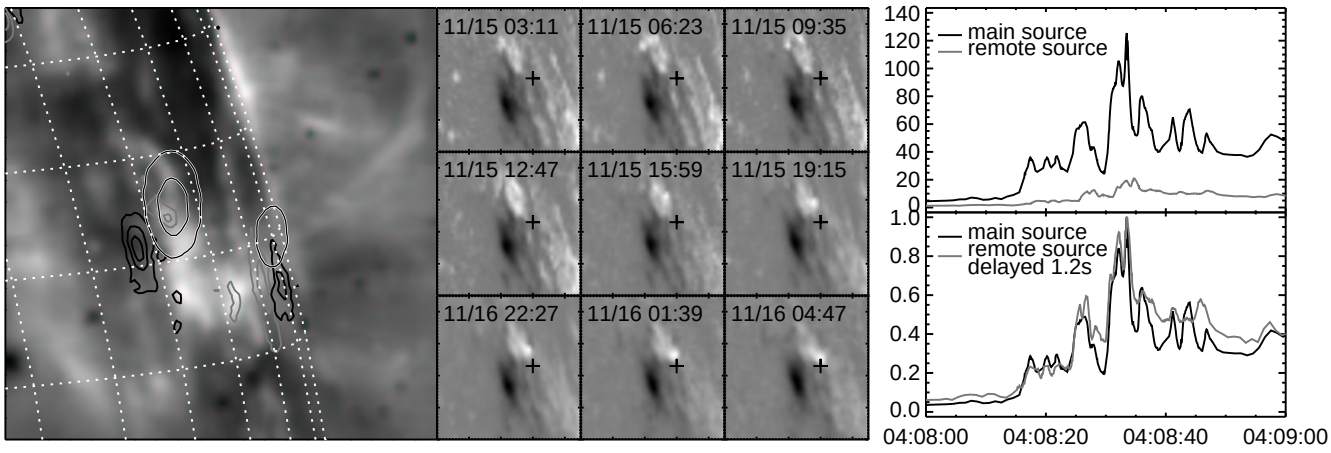

Fig. 3. Time profiles and images of Nov. 16, 1999 event: a)contours of 17GHz image (white line) and MDI image (gray and black line) superposed onto the EIT 195Å image [left panel]; b)a sequence of magnetograms for the leader part of AR 8758 where the main flare site is located [middle panel]; c)comparison of the 17 GHz light curves for the main flare site (black line) and the remote site (gray line) delayed 1.2 s, during the impulse phase of the event [right panel];

be caused by an interaction of magnetic structures either due to an emerging flux or resulting from sideward motion of the coronal loops driven by quasi-rotational photospheric motions.

2. The microwave flaring source consists of two components separated by distances (from 70,000 km to over 10^5 km); the two component sources can be located in separate active regions. The radio emission of the main and remote sources often show opposite senses of circular polarization. Only one source is identified as the main flare site because a bright loop is often observed here in EUV and hard X-rays; by contrast, the remote source is not detected at EUV, soft X-ray or hard X-ray wavelengths. These properties are consistent with the remote radio source being produced by electrons which are accelerated in the main flare site and propagate to the remote flare site where they produce radio emission in strong magnetic fields, but do not deposit a significant amount of energy by precipitation, either because too few electrons reach the remote site or else they mirror in the strong magnetic field there and do not precipitate at the remote site.

3. The radio flare structure consists of a long loop whose footpoints are separated by 110" – 160", and, in addition, a small loop which is the main flare site. This flaring structure is clearly a double-loop configuration of the type discussed earlier by Hanaoka. Hanaoka speculated that emerging flux triggered the interaction between the two loops. The magnetograms acquired every 96 minutes by SOHO/MDI allow us to show that indeed there is a change in magnetic flux in the main flare site just prior to this flare. However, another scenario is also possible for events of this class, namely, the rotation of photospheric magnetic fields around the flare site, possibly producing sheared coronal structures which subsequently flare.

4. During the rise phase of the flare, there seem to exist oscillations in both hard X-ray and microwave domains. The oscillations in the main flare at 17 GHz and in hard X-rays are similar in nature, implying that the same electron population is responsible for the emissions. Transverse oscillations of the main (compact) flare loop are a plausible source of these oscillations. However, they are also observed in the radio light curve of the remote source which is on a different loop: this implies that the injection of nonthermal electrons onto this loop is modulated by oscillations in the main flare loop. The oscillation period allows us to determine the density in the flare loop under the assumption that the oscillation period corresponds to transverse oscillations of the loop at the Alfvén speed.

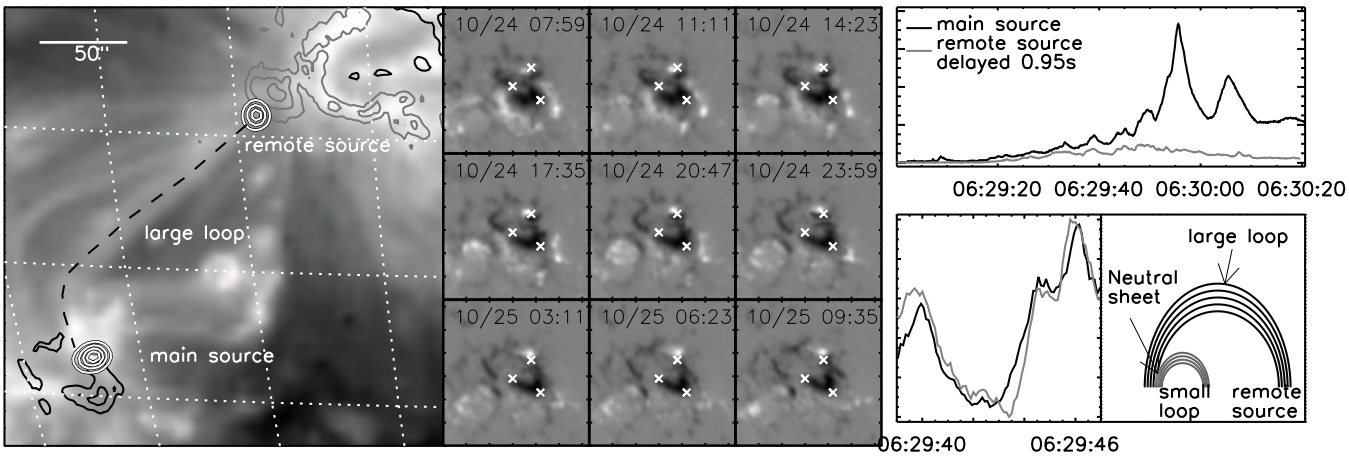

Fig. 4. Time profiles and images of Oct. 25, 1999 event: a)contours of 17GHz image (white line) and MDI image (gray and black line) superposed onto the EIT 195Å image [left panel]; b)a sequence of the magnetograms for the leader part of AR 8741 where the main flare site is located [middle panel]; c)comparison of the 17 GHz light curves for the main flare site (black line) and the remote site (gray line) delayed 0.95 s, during the impulse phase of the event [top -right panel]; d)a schematic model for this class of flares [bottom-right panel].

5. The magnetic connection between the main flare site and the remote site is sometimes broken as in the case of Oct.25 event (Kundu et al 2001) at the time of the main impulsive phase. At this time the main and remote light curves cease to show the same structures with a delay as they do during the rise phase of the flare. This disconnection might be associated with a change of the field lines rooted in the main flare site, such that their magnetic connectivity switches from long connections to the remote site to shorter connections within the main flare site.

ACKNOWLEDGMENTS

This research was supported by NSF grant ATM 99-09809 and NASA grant NAG 5-8192.

REFERENCES

Dulk, G.A., Marsh, K.A.,*ApJ*, **259**, 350, 1982
Hanaoka, Y., *ApJ*, **420**, L37, 1994
Hanaoka, Y., *Sol. Phys.*, **165**, 275, 1996
Hanaoka, Y., *Sol. Phys.*, **173**, 319, 1997
Hanaoka, Y., in Nobeyama Symposium on Solar Physics with Radio Observations, ed. T.S. Bastian, N.Gopalswamy, K.Shibasaki (Nobeyama Radio Observatory), 229, 1999a
Hanaoka, Y., *PASJ*, **51**, 483 1999b
Heyvaerts, J., Priest, E.R., Rust, D.M., *ApJ*, **216**, 123, 1977
Kundu, M.R., Schmahl, E.J., Velusamy, T., Vlahos, L., *A& A*, **108**, 188, 1982
Kundu, M.R., Shevgaonkar, R.K., *ApJ*, **292**, 733, 1985
Kundu, M.R., Grechnev, V.V., Garaimov, V.I., White, S.M., *ApJ*, **563**, 389, 2001